DC Servomotor-based Antenna Positioning Control System Design using Hybrid PID-LQR Controller

Linus A. Aloo[a], **Peter K. Kihato**[b], **Stanley I. Kamau**[c]

[a, b, c] Department of Electrical and Electronic Engineering,
Jomo Kenyatta University of Agriculture & Technology *(JKUAT),*
P.O.BOX 62000-00200, Kenya

Author's E-mail: [a]laloo@jkuat.ac.ke [b]pkihato@jkuat.ac.ke [c]skamau@eng.jkuat.ac.ke

[a] Corresponding Author
E-mail: laloo@jkuat.ac.ke

Sponsor: Jomo Kenyatta University of Agriculture & Technology *(JKUAT)*

Abstract

There are increasing needs to develop control systems that can be used to automatically point Direct Current (DC) servomotor driven parabolic antennas to moving targets, notably in satellite tracking, to maintain the desired line of sight for quality communication. Although many researchers nowadays focus on artificial intelligence techniques, it is reckoned here that a well designed optimal linear controller can still give acceptable results at reduced system cost and complexity. In this paper the design and control of DC servomotor-based antenna positioning system has been addressed and simulated in MATLAB/SIMULINK software. The aim is to minimize deviations from the desired position. The response of the system is analyzed and results are first obtained by using well tuned Proportional-Integral-Derivative (PID) controller. The results of the PID controller are further improved by adding Linear Quadratic Regulator (LQR) which apart from optimizing the system response increases the accuracy of the state variables by estimating the states. It has been shown that the performance of the hybrid PID-LQR controller is much better than that of the PID controller in terms of reduced settling time and overshoot.

Keywords: Antenna-Positioning System, DC servomotor, Linear Quadratic Regulator-LQR, PID Controller

1. INTRODUCTION

Parabolic antennas mounted at earth stations which are commonly used in satellite tracking applications, are prone to suffer from environmental disturbances (Kim, J.K., et al, 2005). For many years, DC servomotor-based controllers have been in use to automatically position the satellite dishes (Hoi, T.V., et al, 2015). Several controller models have been developed over time to solve the problem of antenna pointing in satellite and movable targets tracking using servomechanism (Soltani, M. N., et al, 2010), (Xuan, L., et al, 2009) and (Ahmed, M., et al, 2014). The case of overseas satellite telecommunication is considered by (Soltani, M. N., et al, 2010) where the control system directs on-board motorized antenna towards a selected satellite. Fault Tolerant Control (FTC) system is designed using the ship simulator facility to maintain the tracking functionality. However, the fault estimation has proved to be an extremely challenging task. An overview of most common servomotor-based linear antenna pointing mechanisms: Proportional-Integral (PI), Proportional-Integral-Derivative (PID), Linear Quadratic Gaussian (LQG) modeled and implemented for varied space applications is provided by (Ahmed, M., et al, 2014). PI controllers are easy to implement but take much time to reach set point and have degraded performance under system nonlinearities. LQG controllers are not only optimal but also have the ability to estimate non-measurable states by using observers to reconstruct them and provide better performance in case of wind gusts noise. However, the performances of these methods depend on the accuracy of system models and parameters. Generally, an accurate non-linear model of actual DC motor is difficult to find. Recently, new intelligent control techniques such as Neural Networks, Genetic Algorithms and Fuzzy Logic methods are under research consideration as a viable solution to the problem (Ahmed, M., et al, 2014).

1.1 Problem Formulation

The objective is to design PID and LQR controller for the system under study to meet the following tracking specifications: rise time ($t_r \leq 4\,s$) **,** settling time ($t_s \leq 5s$ and overshoot ($M_p \leq 10\%$). These performance requirements conform to the standards of a practical industrial system.

1.2 System Description

Figure 1 is the control block diagram of the DC servomotor antenna pointing system (Nise, N.S., 2011). The first input to the summer is set position $r(t)$, the desired position at which the azimuth or elevation motor is expected to run to. The second input is the feedback signal, the current position of the respective motor, captured by some feedback sensor like the potentiometer and changed to a summer readable format. The difference between these two inputs, called position error signal $e(t)$, is given to the controller that reads the error signal and produces appropriate output signal, controller output $u(t)$.The controller output then reaches the motor driver, which produces a proportional output to rotate the respective motor in either direction according to the sign of the error signal (positive or negative). As the desired position is approached, the error signal reduces to zero and the motor stops (Ogata, K., 2010).

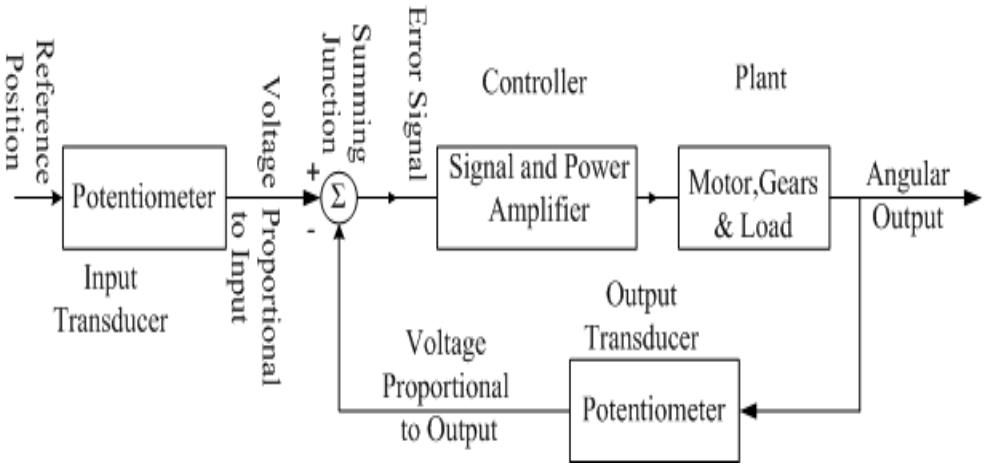

Figure1: Block diagram of antenna control mechanism

2. MATHEMATICAL MODELING OF DC (SERVO) MOTOR SYSTEM

3.

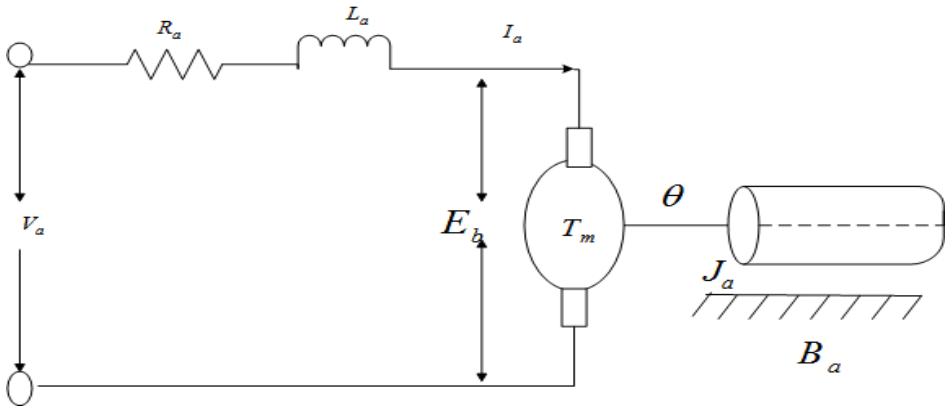

Figure 2: DC motor circuit diagram

Figure 2 represents the DC (servo) motor model (Nise, N.S., 2011) and (Ogata, K., 2010). Reference is made to the parameters defined in table 1 (Xuan, L., et al, 2009). For an armature-controlled separately excited DC motor, the voltage applied to the armature of the motor is varied without changing the voltage applied to the field. Using Kirchhoff's Voltage Law, the output armature voltage $V_a(t)$ and motor torque $T_m(t)$ are related to equation 1:

$$V_a(t) = R_a I_a(t) + L_a \frac{dI_a(t)}{dt} + E_b(t) \tag{1}$$

The motor torque $T_m(t)$ is related to the armature current $I_a(t)$ by a constant factor K_T given in equation 2:

$$T_m(t) = K_T I_a(t) \tag{2}$$

Also, the back electromotive force (e.m.f) $E_b(t)$ is related to the angular velocity by equation 3:

$$E_b(t) = K_T \omega_m(t) = K_T \frac{d\theta}{dt} \tag{3}$$

Table 1: PARAMETERS OF MODEL WITH DC SERVOMOTOR

SCHEMATIC PARAMETERS		
PARAMETER	DEFINITION	AZIMUTH/ ELEVATION
a	Power Amplifier Pole	100
a_m	Motor and Load Pole	1.71
B_a	Motor Dampening Constant[Nms/rad]	0.01
B_L	Load Dampening Constant[Nms/rad]	1
B_m	Equivalent viscous friction coefficient [Nms/rad]	0.02
J_a	Motor Inertial Constant[Kgm^2]	0.02
J_L	Load Inertial Constant[Kgm^2]	1
J_m	Equivalent moment of inertia[Kgm2]	0.03
K	Preamplifier Gain	_
K_1	Power Amplifier Gain	100
K_B	Back emf Constant[Vs/rad]	0.5
K_g	Gear Ratio	0.1
K_m	Motor and Load Gain	2.083
K_{pot}	Potentiometer Gain	0.318
K_T	Motor Torque Constant[Nm/A]	0.5
L_a	Motor Armature Inductance[H]	0.45
N	Turns on Potentiometer	10
N_1, N_2, N_3	Gear Teeth (Respectively)	25,250,250
Ra	Motor Armature Resistance[Ω]	8
V	Voltage across Potentiometer[V]	10

Newton's Law and Kirchhoff's Law give equations 4 and 5:

$$J_a \frac{d^2\theta}{dt^2} + B_a \frac{d\theta}{dt} = K_T I_a(t) \tag{4}$$

$$L_a \frac{dI_a(t)}{dt} + R_a I_a(t) = V_a(t) - K_T \frac{d\theta}{dt} \tag{5}$$

Applying Laplace transform to equations 4 and 5 assuming zero initial conditions gives equations 6 and 7:

$$J_a s^2 \theta(s) + B_a s \theta(s) = K_T I_a(s) \tag{6}$$

$$L_a s I_a(s) + R_a I_a(s) = V_a(s) - K_T s\theta(s) \tag{7}$$

Making current the subject in equation 7 and substituting in equation 6, generates equation 8:

$$J_a s^2\theta(s) + B_a s\theta(s) = K_T \frac{V_a(s) - K_T s\theta(s)}{R_a + L_a s} \tag{8}$$

From equation 8, the transfer function from the input voltage, $V_a(s)$ to the output angle θ directly follows equation 9:

$$G_a(s) = \frac{\theta(s)}{V_a(s)} = \frac{K_T}{s[(R_a + L_a s)(J_m s + B_m) + K_T K_B]} \tag{9}$$

Figure 3 is a block diagram of DC servomotor system showing elements of the transfer function.

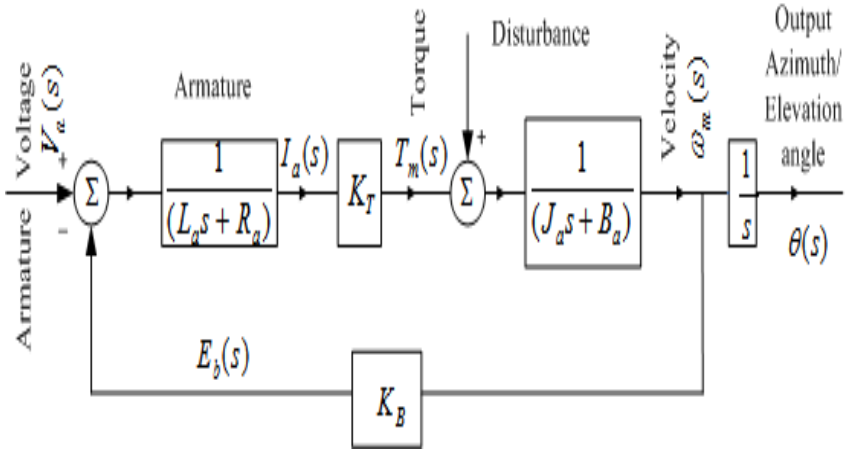

Figure 3: Block diagram of separately excited DC (servo) motor

The transfer function from input voltage, $V_a(s)$ to angular velocity, $\omega_m(s)$ is realized as in equation 10:

$$G_a(s) = \frac{\omega_m(s)}{V_a(s)} = \frac{K_T}{[(R_a + L_a s)(J_m s + B_m) + K_T K_B]} \tag{10}$$

State-space form of the above equations is expressed by choosing the rotating speed, output position and electrical current as state variables and the voltage as an input. The output is chosen to be the rotating speed and position. The Linear-Time-Invariant (LTI) system is given generally by equation 11:

$$\begin{cases} \dot{x}(t) = Ax(t) + Bu(t) \\ y(t) = Cx(t) + Du(t) \end{cases} \tag{11}$$

where A is an nxn state matrix, B is an nxr input matrix, C is mxn output matrix, D is an mxr matrix, $x(t)$ is an n-state vector and u(t) is r-control vector (Orji, W.U., et al, 2015). Equation 12 & 13 indicate the state-space representation of DC motor speed/position control:

$$\begin{bmatrix} \frac{di_a}{dt} \\ \frac{d\omega_r}{dt} \\ \frac{d\theta_m}{dt} \end{bmatrix} = \begin{bmatrix} -\frac{R}{L} & -\frac{K_b}{L} & 0 \\ \frac{K_m}{J} & -\frac{B}{J} & 0 \\ 0 & 1 & 0 \end{bmatrix} \begin{bmatrix} i_a \\ \omega_r \\ \theta_m \end{bmatrix} + \begin{bmatrix} \frac{1}{L} \\ 0 \\ 0 \end{bmatrix} V_a \tag{12}$$

$$y = [010] \begin{bmatrix} i_a \\ \omega_r \\ \theta_m \end{bmatrix} + [0] V_a \tag{13}$$

Using values from Table I in equations 12 & 13 and comparing with equation 11 gives equation 14:

$$A = \begin{bmatrix} -17.78 & -1.111 & 0 \\ 25 & -0.5 & 0 \\ 0 & 1 & 0 \end{bmatrix}, B = \begin{bmatrix} 2.22 \\ 0 \\ 0 \end{bmatrix}, C = [0\ 1\ 0] \text{ and } D = [0] \tag{14}$$

4. PROPORTIONAL-INTEGRAL-DERIVATIVE (PID) CONTROLLER

PID controllers are implemented in most industrial processes. This is because they are low cost, can usually provide good closed-loop response characteristics, tuned using relatively simple rules and are relatively easy to construct. Control signal is the sum of three components: proportional, integral and derivative gain scaling factors (Chishti, A.R., et al, 2014). The structure of PID controller is shown in figure 4.

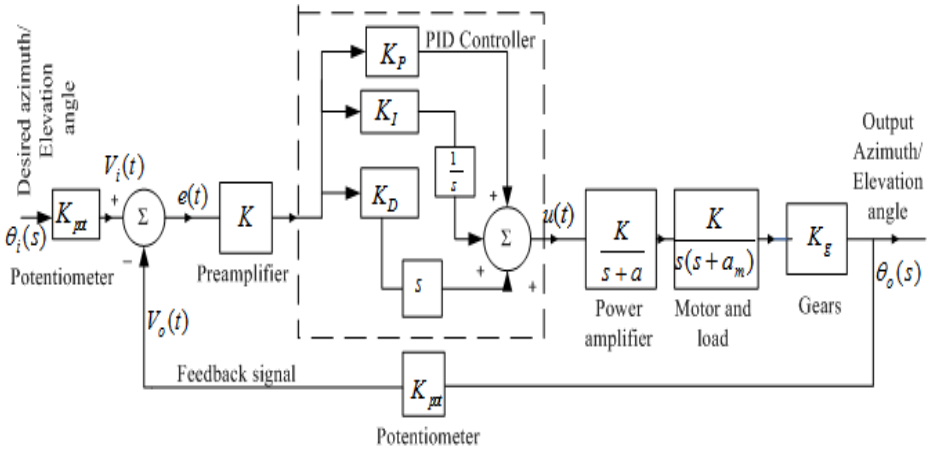

Figure 4: Block diagram of Antenna Azimuth PID controller

To derive the closed-loop system transfer function without the (PID) compensator, the following assumptions are made (Xuan, L., et al, 2009):

- That power amplifier and preamplifier transfer functions are accurate and saturation is never reached.
- No disturbances in the signals sent between system parts.

From equation 9, equation 15 is obtained:

$$E_a(s) = \frac{[(J_m s^2 + B_m s)(R_a + L_a s) + K_T K_B s]}{K_T} \theta_m(s) \tag{15}$$

In a fixed field motor it is assumed that $K_T = K_B$, $R_a >> L_a$ and equation 15 simplifies to equation 16:

$$\frac{\theta_m(s)}{E_a(s)} = \frac{\frac{K_T}{JR_a}}{s(s + \frac{B_m R_a + K_T K_B}{JR_a})} \tag{16}$$

The system parameters including the DC servomotor are given in table 1 (Xuan, L., et al, 2009), (Nise, N.S., 2011). Using gear ratio the transfer function relating load displacement to motor armature voltage is equation 17:

$$\frac{\theta_o(s)}{E_a(s)} = 0.1 \frac{K_m}{s(s + a_m)} = \frac{0.2083}{s(s + 1.71)} \tag{17}$$

The open-loop transfer function for output angular velocity ($\omega_o(t)$) without feedback (Chishti, A.R., et al, 2014) is given in equation 18:

$$G_a(s) = \frac{\omega_o(s)}{V_p(s)} = \frac{20.83}{s^2 + 101.71s + 171} \tag{18}$$

The closed-loop transfer function without the PID compensator (Chishti, A.R., et al, 2014) is found by using equation 18 and the block diagram reduction (Nise, N.S.,2011) to get equation 19:

$$\frac{\theta_o(s)}{\theta_i(s)} = \frac{6.63K}{s^3 + 101.71s^2 + 171s + 6.63K} \tag{19}$$

According to Routh-Herwitz criterion (Nise, N.S., 2011), (Ogata, K., 2010), the system will give stable response with the value of "K" in the range 0 < K < 2623. Here, the gain value taken is 100 which had been chosen to be equal to that of the power amplifier for design convenience and to reduce energy consumption while still falling within the stability range (Chishti, A.R., et al, 2014). Equation 19 becomes equation 20:

$$\frac{\theta_o(s)}{\theta_i(s)} = \frac{663}{s^3 + 101.71s^2 + 171s + 663} \tag{20}$$

State-space of closed-loop transfer function of antenna azimuth position control is represented as in equation (21)

$$A = \begin{bmatrix} -101.7100 & -171.0000 & -663.0000 \\ 1.0000 & 0 & 0 \\ 0 & 1 & 0 \end{bmatrix} B = \begin{bmatrix} 1 \\ 0 \\ 0 \end{bmatrix} a \text{ , } C = \begin{bmatrix} 0 & 0 & 663 \end{bmatrix} \text{ and } D = \begin{bmatrix} 0 \end{bmatrix} \tag{21}$$

The PID controller in parallel form (Kumar, P.R., et al, 2014) is equation 22:

$$U(t) = K_p e(t) + K_I \int e(t) + K_D \frac{de(t)}{dt} \tag{22}$$

where K_P, K_I and K_D are proportional, integral and derivative gains and $e(t)$ = error. The Transfer function of PID controller in Frequency domain is represented in equation 23:

$$\frac{U(s)}{E(s)} = K_P + \frac{K_I}{s} + K_D s \tag{23}$$

Using PID, closed-loop transfer function, (Chishti, A.R., et al, 2014) is equation 24:

$$\frac{\theta_o(s)}{\theta_i(s)} = \frac{663K_D s^2 + 663K_P s + 663K_I}{s^4 + 101.71s^3 + (171 + 663K_D)s^2 + 663K_P s + 663K_I} \tag{24}$$

The values of proportional (K_P), integral (K_I) and derivative (K_D) gains are obtained using Ziegler Nichols tuning algorithm. This method gives automatic oscillation of the process to compute the three gain constants. Ziegler-Nichols presented two methods: Step response method and Frequency response method (Kumar, P.R., et al, 2014). In this paper frequency response method was used to obtain the preliminary gain values of the PID controller as follows: $K_P = 15$, $K_D = 90$ and $K_I = 0.625$. However, since these initial gain constants depicted high overshoots, the final PID controller gain parameters which gave the most appropriate response and thus meeting the design constraints were obtained as follows: $K_P = 18$, $K_I = 4$ and $K_D = 2$.

5. LINEAR QUADRATIC REGULATOR (LQR) CONTROLLER & PID-LQR DESIGN

Linear Quadratic Regulator (LQR) design technique is used in modern optimal control theory and has been widely used in many control applications besides Proportional Integral Derivative (PID) because of its stability (Frank, L., et al, 2012). It uses state-space approach to analyze and control an LTI system whose general model was represented in equation 11. To start LQR design the following assumptions are made:

1. Plant model defined by equation 11 is perfectly known.
2. All states are directly measurable (available for feedback).

If assumption 1 is not true (the model has uncertainties), robust control is preferred. If assumption 2 is not true (only the output is measurable), then an observer is required, in which case, the system must be observable. The LQR method is used to achieve acceptable system performance by minimizing the performance index (cost) value J, (Yu, G.R. & Hwang, R.C, 2004), defined for t_f=∞ (steady-state case) by equation (25):

$$J = \frac{1}{2}\int_{t_0}^{\infty} (x^T(t)Qx(t) + u^T(t)Ru(t))dt \tag{25}$$

where $R = R^T > 0,$ is weighting factor of control variables (positive definite matrix) and $Q = Q^T \geq 0$ is weighting factor of states (positive semi-definite matrix). The LQR control technique involves choosing a control law $u(t) = -Kx(t)$ in which $K = R^{-1}B^T P$ is the LQR state feedback control gain which is used to stabilize the origin (i.e. regulating x to zero). *P* is the unique, positive semi-definite solution of the algebraic Riccati equation (ARE) (Frank, L., et al, 2012), (Yu, G.R. & Hwang, R.C, 2004), given by equation 26:

$$A^T P(t) + P(t)A + Q - P(t)BR^{-1}B^T P(t) = 0 \tag{26}$$

For $t_f = \infty$, $P(t) = P$ (constant). Figure 5 shows block diagram of Linear Quadratic Controller for DC servomotor system.

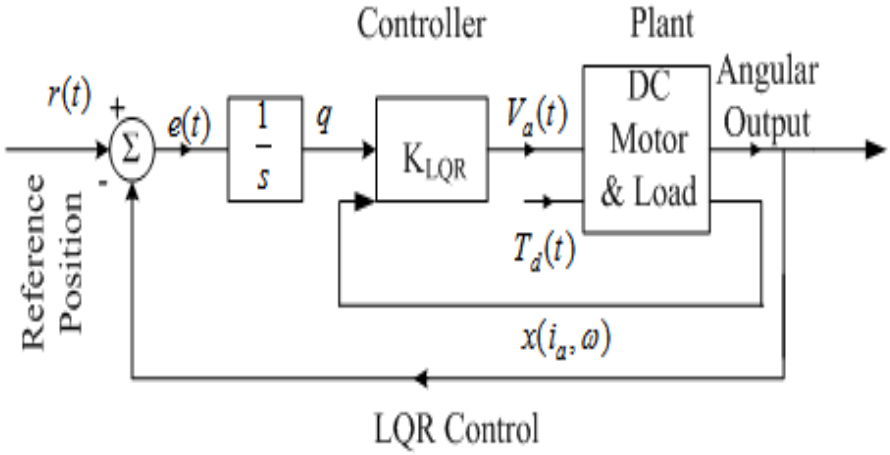

Figure 5: Linear Quadratic Regulator (LQR) control system

To design LQR controller, the first step is to select the weighting matrices Q and R. The value R weight inputs more than the states while the value of Q weight the states more than the inputs (Burns, R.S, 2001). Next, the constant feedback gain vector K is computed using MATLAB 'lqr' command given A, B, Q and R and the closed-loop system step responses found by simulation. To formulate LQR-based optimal PID controller, we utilized the second order system transfer function, equation 18, given in figure 6, with known open loop damping ratio and natural frequency i.e. $\xi^{ol} = 3.899$, $\omega_n^{ol} = 13.07\, rad/s$,.

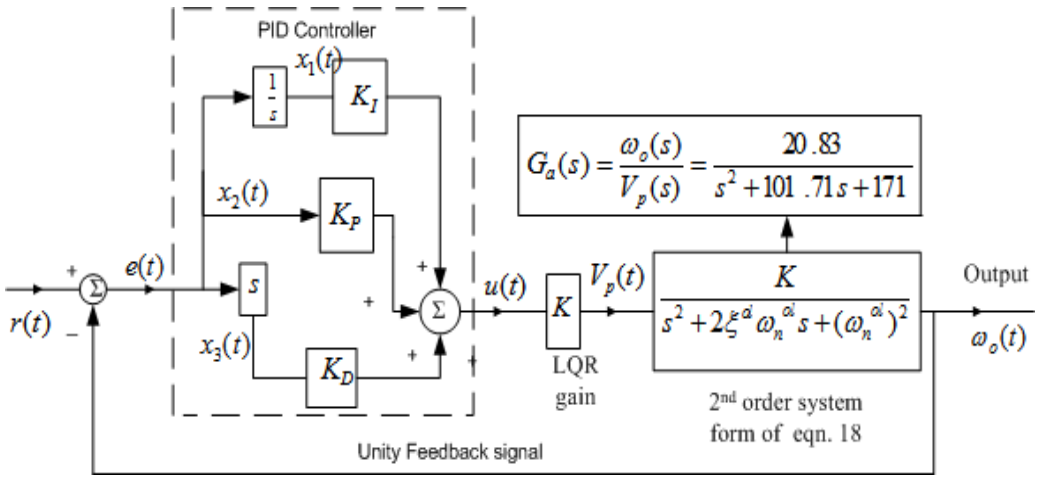

Figure 6: LQR Formulation of PID controller for second order process

In this approach we assumed the error, its rate and integral as the state variables and designed the optimal state-feedback controller gains as the PID controller parameters. Let the state variables be defined as:

$$\left.\begin{aligned} x_1 &= \int e(t)dt \\ x_2 &= e(t) \\ x_3 &= \frac{de(t)}{dt} \end{aligned}\right\} \tag{27}$$

From block diagram of Figure 6 and equation 18, the state-space formulation is given in equation 28, from which values of A and B can be obtained as before:

$$\begin{bmatrix} \dot{x}_1 \\ \dot{x}_2 \\ \dot{x}_3 \end{bmatrix} = \begin{bmatrix} 0 & 1 & 0 \\ 0 & 0 & 1 \\ 0 & -171.00 & -101.71 \end{bmatrix} \begin{bmatrix} x_1 \\ x_2 \\ x_3 \end{bmatrix} + \begin{bmatrix} 0 \\ 0 \\ -K \end{bmatrix} u \tag{28}$$

The solution of ARE is obtained by setting the elements of the P matrix and weighting matrix Q in the form of equation 29:

$$P = \begin{bmatrix} P_{11} & P_{12} & P_{13} \\ P_{12} & P_{22} & P_{23} \\ P_{13} & P_{23} & P_{33} \end{bmatrix}, Q = \begin{bmatrix} Q_1 & 0 & 0 \\ 0 & Q_2 & 0 \\ 0 & 0 & Q_3 \end{bmatrix} \tag{29}$$

$$\mathrm{K} = R^{-1}B^T P = R^{-1}\begin{bmatrix} 0 & 0 & -K \end{bmatrix} \begin{bmatrix} P_{11} & P_{12} & P_{13} \\ P_{12} & P_{22} & P_{23} \\ P_{13} & P_{23} & P_{33} \end{bmatrix} = R^{-1}K\begin{bmatrix} P_{13} & P_{23} & P_{33} \end{bmatrix} = -[K_I \; K_P \; K_D] \tag{30}$$

$$\mathrm{u(t)} = -Kx(t) = -[-K_I \; -K_P \; -K_D] \begin{bmatrix} x_1(t) \\ x_2(t) \\ x_3(t) \end{bmatrix} = K_I \int e(t) + K_p e(t) + K_D \frac{de(t)}{dt} \tag{31}$$

The above formulation, equations 30 and 31, clearly shows that with judicious choice of weighting matrices {Q, R}, a PID controller can easily be tuned which preserves the achievable performance of an LQR. The final values for hybrid PID-LQR controller were obtained as $K = 2$, $K_p = 3$, $K_I = 5$ and $K_D = 1$. The LQR controller was designed with the aid of MATLAB code. It is necessary to achieve proper choice of the two parameters, R and Q, which will balance the relative importance of the control effort (u) and error (deviation from 0), respectively, in the cost function. In order to improve the design and tune the response, various Q matrices and R values were tried. For instance, Q matrices, [1 0; 0 10] and [1 0; 100] and for R, 0.1 and 0.01 were tried. It was found that increasing the (1, 1) and (2, 2) elements of the Q matrix made the settling and rise times to go down, and lowered the angle the motor moved. In addition, it was noted that if the values of the elements of Q were increased even higher, the response could be improved even more by reducing the tracking error but this would require greater control effort u which corresponds to greater cost (more energy, larger actuator, etc.). The value of K for LQR alone that gave the desired optimized performance was finally obtained as $K = [-0.6435 \quad 169.06950 \quad 7.07]$, which satisfied the transient design requirements.

6. SIMULINK MODEL

The SIMULINK model for the designed PID, LQR and hybrid PID-LQR control systems created in MATLAB software for conducting the simulations is shown in figure7.

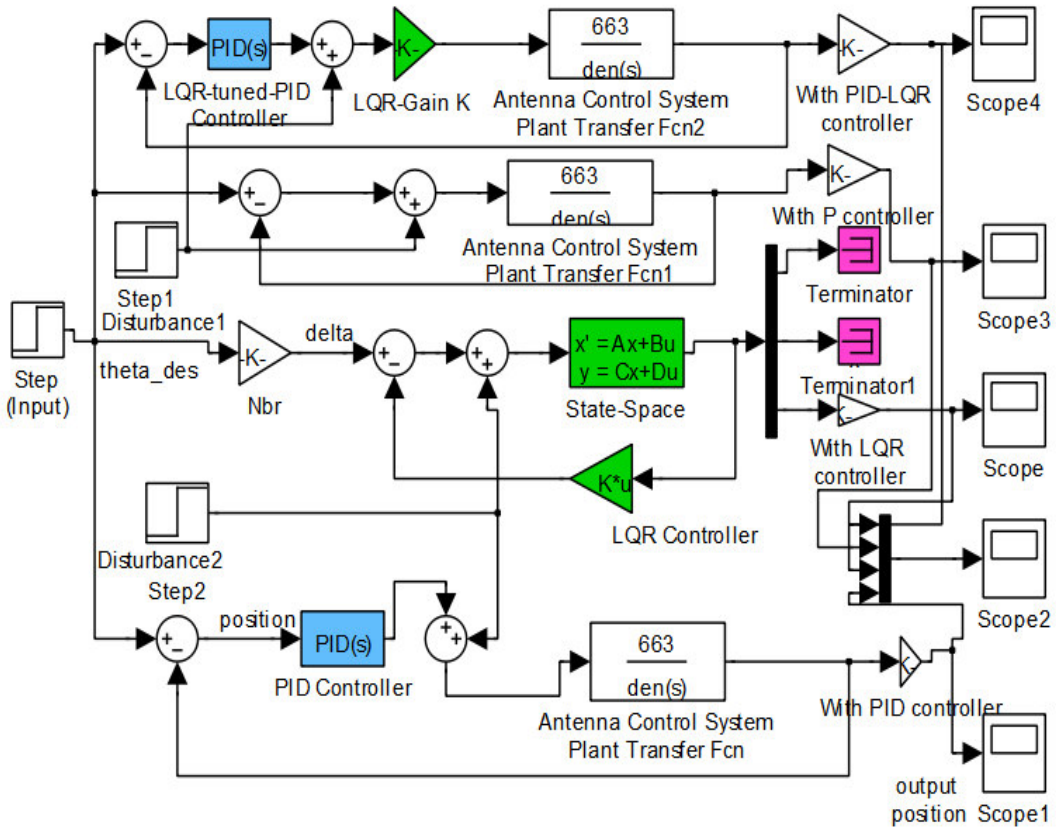

Figure7: PID, LQR & Hybrid PID-LQR Control Simulink model layout

The controller is taken as a PID controller in one case and as PID-LQR in another case. A step input signal was taken as the reference and applied to the plant transfer function and state-space system.

7. RESULTS AND DISCUSSIONS

The proposed PID-LQR Control system has been addressed by simulation. Further, it has been compared with the PID controller in order to evaluate its performance. Response of closed-loop antenna position control system with unity gain Proportional (P) controller is shown in figure 8, from which it is noticed that the response is not good due to unacceptable overshoot. In figure 9, the step response of the system has been improved with inclusion of PID controller which though significantly reduces the value of steady-state error, the rise time and the settling time, is still not satisfactory on account of high overshoot.

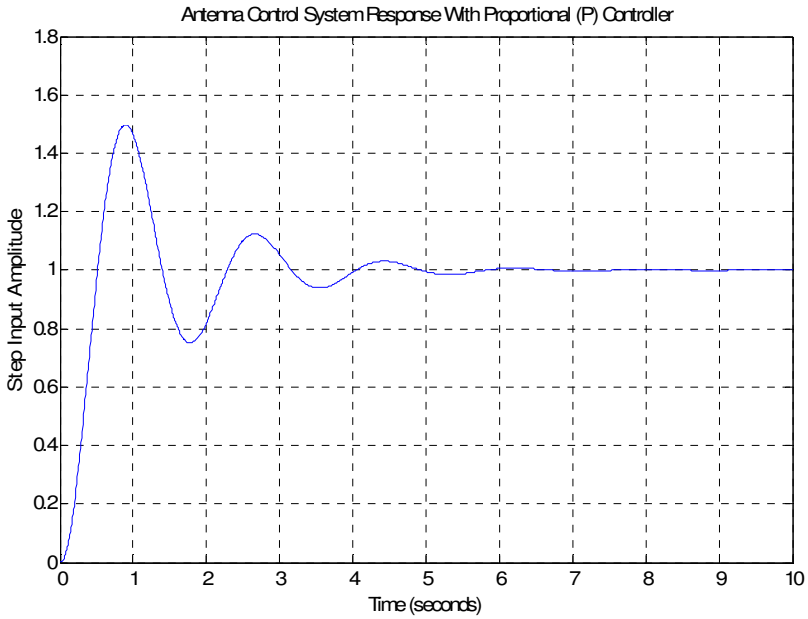

Figure8: Step response of system with Proportional (P) controller

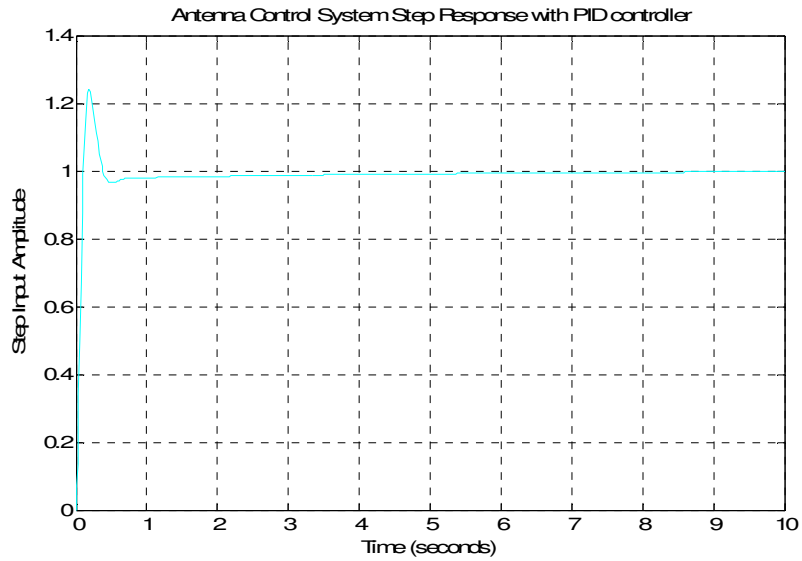

Figure 9: Step response of system with PID controller

Figure 10 indicates plot of closed-loop system state variables upon which LQR control design is applied.

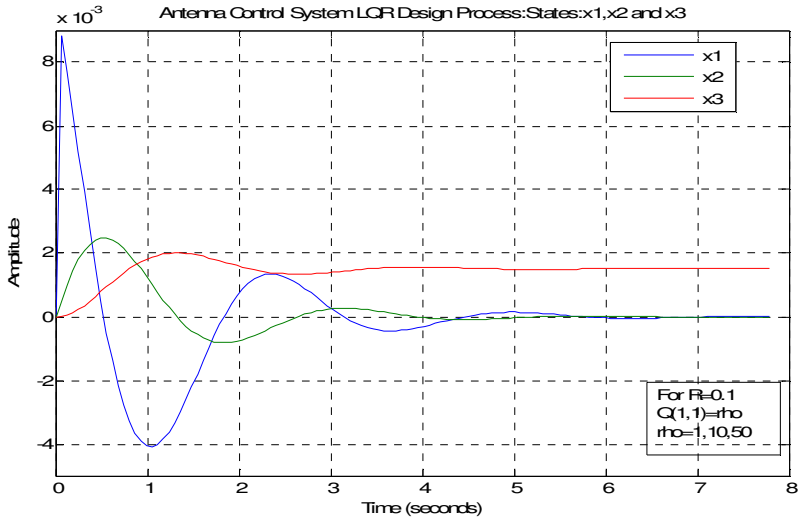

Figure10: Closed-loop states for use in LQR control design

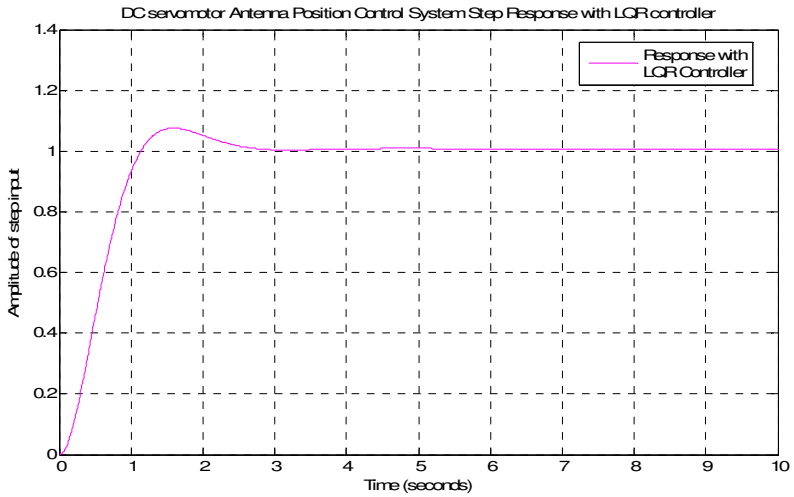

Figure 11: Step response of antenna control system using LQR control

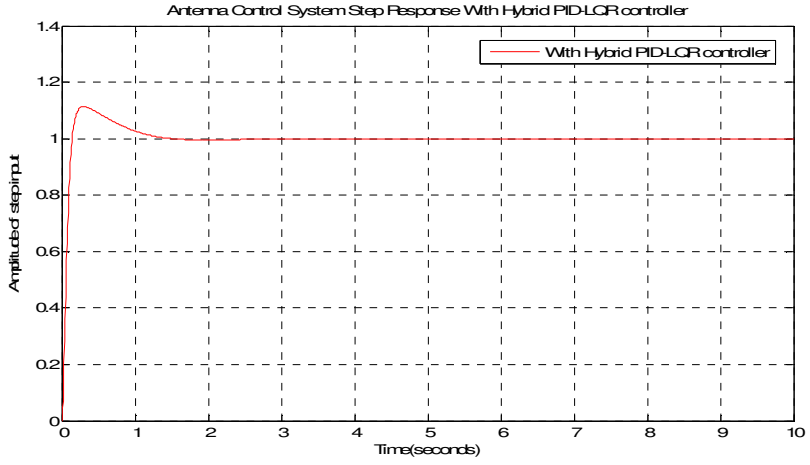

Figure 12: Step response of antenna control system using PID-LQR controller

Figure 11 shows the system response by using LQR Controller while figure 12 shows response with hybrid PID-LQR. Figure 13 shows on the same axes, the comparison of the system step response with unity gain Proportional (P) controller and with the PID, LQR and combined PID-LQR controllers.

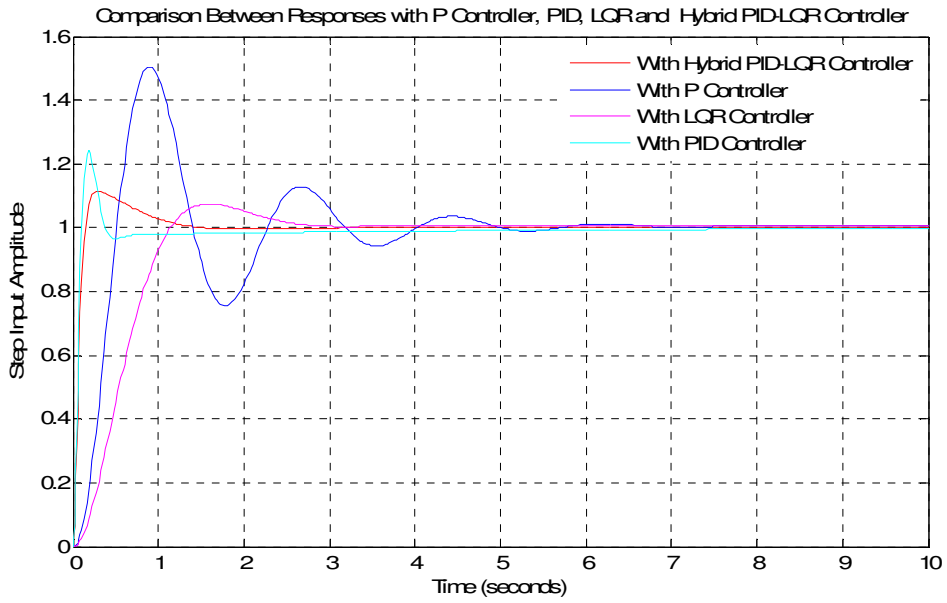

Figure 13: Step Responses with Proportional, PID, LQR and hybrid PID-LQR Controller

A single MATLAB m-file was also developed to simulate the performance of the PID-LQR control technique for tracking set point commands and reducing the sensitivity of ω_{ref} to load disturbances. A feed forward control design was also included.

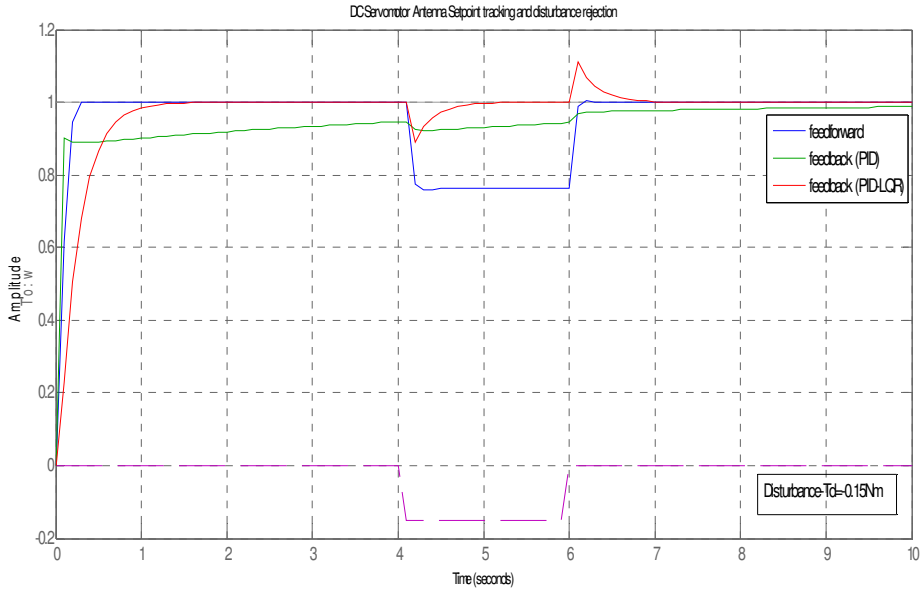

Figure 14: PID-LQR step response with disturbance at t=4s.

The torque T_d models load disturbances (changes in the torque opposed by the motor load). The controller must minimize the position/speed variations induced by such disturbances. Figure 14 shows the response to

a step command $\omega_{ref} = 1$ with a disturbance $T_d = -0.15Nm$ between $t = 4\,\text{sec}$ and $t = 6\,\text{sec}$. Once again, thanks to its additional degrees of freedom, the PID-LQR compensator performs best at rejecting load disturbances compared to PID controller. Clearly, feed forward control handles load disturbances poorly. From the simulation results it is seen that LQR provides response with faster settling times and reduced overshoots when compared to PID controller. The maximum overshoot with LQR is minimized to less than 4.0% while it was 23.5% with PID alone. The rise time is 0.2 seconds with PID controller and 0.9 seconds with the LQR for response to transit from 10% to 90% of the steady state value. Moreover, in addition to the strengths of LQR over PID, the combined PID-LQR registered the best overall performance of 0.2seconds rise time, 5.0 % overshoot and 1 second settling time.

8. CONCLUSION AND FUTURE WORK

A PID-LQR controller for DC servomotor based antenna pointing system has been designed, studied and the performance was evaluated by simulation. The LQR satisfied all the design requirements and results indicated significant improvement from the hybrid combination of PID with LQR in maintaining performance of approximate zero overshoot and minimum stabilizing time as compared to the classical PID controller which despite having lower rise time, suffered a lot in terms of registering higher overshoots and settling times. The objectives were met in both design approach and software simulations. Future work is to use Fuzzy Logic and Neural Network based techniques to solve for the same problem and investigate on whether better results could be achieved.

REFERENCES

[1] Kim, J.K., Cho K.R. & Jang, C. S. (2005). Fuzzy control of data link antenna control system for moving vehicles. ICCAS.

[2] Hoi, T.V., Xuan, N. T. & Duong, B. G. (2015). Satellite tracking control system using Fuzzy PID controller. VNU Journal of Science: Mathematics and Physics, vol. 31, no. 1, pp. 36-46.

[3] Soltani, M. N., Zamanabadi, R. & Wisniewski, R. (2010). Reliable control of ship-mounted satellite tracking antenna. IEEE Transactions on Control Systems Technology, p. 99.

[4] Xuan, L., Estrada, J. & Di Giacomandrea, J. (2009). Antenna azimuth position control system analysis and controller implementation. Design Problem.

[5] Ahmed, M., Mohd Noor, S.B., Hassan M. K. & Che Soh, A. B. (2014). A Review of Strategies for Parabolic Antenna Control. Australian Journal of Basic and Applied Sciences, vol. 8(7), pp. 135-148.

[6] Nise, N.S. (2011). Control System Engineering. John Wiley & Sons, 6th Edition.

[7] Ogata, K. (2010), Modern Control Engineering, Prentice-Hall Inc. USA, 5th Edition, p.95-96.

[8] Orji, W.U., Christian, M. C., Egbunonu, C. I. & Okorie, C. K. (2015). Performance Analysis of Linear Quadratic Regulator Controller Design Techniques for Optimal Servomotor Speed Control. International Journal of Scientific & Engineering Research, Volume 6, Issue 4.

[9] Chishti, A.R., Bukhari, S.F., Khaliq, H.S., Khan M.H., & Bukhari, S.Z. (2014). Radio Telescope Antenna Azimuth Position Control System Design and Analysis in MATLAB/Simulink using PID&LQR Controller. The Islamia University of Bahawalpur, Pakistan.

[10] Kumar, P.R. & Babu, V.N. (2014). Position Control of Servo Systems using PID Controller Tuning with Soft Computing Optimization Techniques. International Journal of Engineering Research & Technology (IJERT), vol. 3, pp. 976-980.

[11] Frank, L., Vrabie, L. D. & Syrmos, V. L. (2012). Optimal Control. 3rd Edition, New Jersey, USA, John Wiley and Sons.

[12] Yu, G.R. & Hwang, R.C. (2004). Optimal PID speed control of brush less DC motors using LQR approach. In Proc. IEEE International Conference on Man and Cybernetics, pages 473–478, Hague, Netherlands.

[13] Burns, R. S. (2001). Advanced Control Engineering. Butterworth Heinemann, Jordan Hill, Oxford, ISBN 0750651008, pg 274-285.